The Convective Electric Field Influence on the Cold Plasma and Diamagnetic Cavity of Comet 67P

Niklas Edberg, Anders Eriksson, Erik Vigren, Fredrik Johansson, Charlotte Goetz, Hans Nilsson, Nicolas Gilet, Pierre Henri

The Astronomical Journal, 158:71 (6pp), 2019 August https://doi.org/10.3847/1538-3881/ab2d28

The Convective Electric Field Influence on the Cold Plasma and Diamagnetic Cavity of Comet 67P

Niklas J. T. Edberg[1], Anders I. Eriksson[1], Erik Vigren[1], Fredrik L. Johansson[1], Charlotte Goetz[2], Hans Nilsson[3,4], Nicolas Gilet[5], and Pierre Henri[5]
[1] Swedish Institute of Space Physics, Lägerhyddsvägen 1, SE-75121 Uppsala, Sweden; ne@irfu.se
[2] Institut für Geophysik und extraterrestrische Physik, Technische Universität Braunschweig, Germany
[3] Swedish Institute of Space Physics, PO Box 812, SE-98128 Kiruna, Sweden
[4] Luleå University of Technology, Department of Computer Science, Electrical and Space Engineering, Rymdcampus 1, SE-98128, Kiruna, Sweden
[5] Laboratoire de Physique et Chimie de l'Environnement et de l'Espace (LPC2E), CNRS, Orléans, France
Received 2019 March 20; revised 2019 June 24; accepted 2019 June 25; published 2019 July 19

Abstract

We studied the distribution of cold electrons (<1 eV) around comet 67P/Churyumov–Gerasimenko with respect to the solar wind convective electric field direction. The cold plasma was measured by the Langmuir Probe instrument and the direction of the convective electric field $\boldsymbol{E}_{\rm conv} = -\boldsymbol{v} \times \boldsymbol{B}$ was determined from magnetic field ($\boldsymbol{B}$) measurements inside the coma combined with an assumption of a purely radial solar wind velocity $\boldsymbol{v}$. We found that the cold plasma is twice as likely to be observed when the convective electric field at *Rosetta*'s position is directed toward the nucleus (in the $-\boldsymbol{E}_{\rm conv}$ hemisphere) compared to when it is away from the nucleus (in the $+\boldsymbol{E}_{\rm conv}$ hemisphere). Similarly, the diamagnetic cavity, in which previous studies have shown that cold plasma is always present, was also found to be observed twice as often when in the $-\boldsymbol{E}_{\rm conv}$ hemisphere, linking its existence circumstantially to the presence of cold electrons. The results are consistent with hybrid and Hall magnetohydrodynamic simulations as well as measurements of the ion distribution around the diamagnetic cavity.

Key words: comets: individual (67P) – magnetic fields – plasmas – space vehicles: instruments

1. Introduction

The ionospheric plasma of comet 67P/Churyumov–Gerasimenko (hereafter 67P) includes several electron populations—a hot, a warm, and a cold population (Broiles et al. 2015; Eriksson et al. 2017; Engelhardt et al. 2018). These populations stem from the process of ionization of neutrals in the coma through photoionization or electron impact ionization (Broiles et al. 2015; Edberg et al. 2015; Johansson et al. 2017; Heritier et al. 2018), and are altered through charge exchange processes including the solar wind plasma (Simon Wedlund et al. 2017). Photoionization creates free electrons with an energy of about 10 eV, and electrons from impact ionization have similar "warm" energy. At 67P, a significant amount of hot electrons, i.e., an energy of ∼100 eV, was present, believed to be heated through wave–particle interaction (Broiles et al. 2016; André et al. 2017; Karlsson et al. 2017) or through the interaction with the solar wind (Broiles et al. 2015, 2016; Edberg et al. 2016a, 2016b). Cold electrons with an energy <1 eV were also observed, believed to have been cooled through collisions with neutrals before they reached *Rosetta*, and possibly also affected by ambipolar electric fields (Madanian et al. 2016; Eriksson et al. 2017; Gilet et al. 2017; Vigren et al. 2017; Engelhardt et al. 2018; Vigren & Eriksson 2019).

Eriksson et al. (2017) and Engelhardt et al. (2018) found that the cold electrons were present throughout most of the *Rosetta* mission but were observed more frequently toward perihelion, when the outgassing rate and the plasma density were higher. The cold plasma was also observed to appear in pulses, or filaments, which is in agreement with simulations in which the cold plasma breaks up into such structures outside of 30–50 km from the nucleus (Koenders et al. 2015). The cold electrons were also found more often close to the electron collision boundary, toward the dayside (low solar zenith angle, SZA), and at low latitudes, which coincides with where the neutral density is higher.

In this paper the focus is on the distribution of this cold electron population with the solar wind convective electric field. While, e.g., ambipolar electric fields, set up by charge separations in the coma, affect the plasma locally, the hypothesis here is that the convective electric field of the solar wind, in the rest frame of the comet, affects the plasma environment globally.

The solar wind and its frozen-in magnetic field interacts with the comet to cause a variety of effects. One important parameter of the solar wind is the orientation of the convective electric field

$$\boldsymbol{E}_{\rm conv} = -\boldsymbol{v} \times \boldsymbol{B}, \quad (1)$$

where $\boldsymbol{v}$ is the solar wind velocity and $\boldsymbol{B}$ is the magnetic field. We define two reference frames to be used in this paper: in the cometary solar equatorial (CSEQ) reference frame the $+x$-axis points from the comet to the Sun, the $+z$-axis is the component toward the north pole of the Sun of date orthogonal to the $+x$-axis, and the $+y$-axis completes the right-handed reference frame and the origin of this frame is the center of mass of the comet. The cometary solar electric (CSE) frame is used to describe the measurements in relation to the solar wind convective electric field. In this frame the origin is again the center of mass of the comet and the $+x$-axis points from the comet to the Sun, but the $+y$-axis is aligned with the local magnetic field direction and the $+z$-axis is thus parallel to $\boldsymbol{E}_{\rm conv}$. Simulations of the plasma environment, which take into account kinetic effects, do indicate that the cometary electrons in the coma are preferentially traveling in a direction antiparallel to $\boldsymbol{E}_{\rm conv}$ (Koenders et al. 2015; Deca et al. 2017). The electrons follow the deflected solar wind ions rather than

the picked up cometary ions, and are thus on a global scale affected by the convective electric field.

Moreover, in the inner parts of the cometary plasma environment is the so-called diamagnetic cavity (e.g., Biermann et al. 1967; Goetz et al. 2016). This is a void in the plasma environment characterized by a negligible magnetic field, which was observed very sporadically, or pulse-like, in the *Rosetta* data. Standard theory explains that the diamagnetic cavity as due to a pressure balance between the external magnetic pressure and the internal ion-neutral drag force, which was supported by the measurements of similar ion and neutral velocity at comet 1P/Halley (Cravens et al. 1987) and some *Rosetta* studies have used this model also for 67P (Timar et al. 2017). However, other *Rosetta* measurements have led to questioning the applicability of this theory as the ion and neutral velocity were found to differ significantly to each other (Odelstad et al. 2018). Hence, the physics of this region is still under debate. Based on an observed correlation between cavity observations and vicinity to the electron-neutral decoupling distance, Henri et al. (2017) suggested that electron-neutral collisions were more important than ion-neutral collisions, while Timar et al. (2017) did indeed find a good correlation between the observed radial distance of the cavity to that predicted by the ion-neutral drag force model. Odelstad et al. (2018) also found that cold electrons were always present inside the diamagnetic cavity, which leads us to investigate if the appearance of the diamagnetic cavity is also dependent on the convective electric field direction.

2. Data

We use data from the Langmuir probe (LAP) and magnetometer (MAG) instrument within the *Rosetta* plasma consortium (RPC; Eriksson et al. 2007; Glassmeier et al. 2007). LAP uses two spherical TiN-coated probes with diameters of 50 mm mounted on stubs on two separate booms. The booms extend approximately 1.6 and 2.2 m away from the spacecraft body, respectively. Onboard electronics steer the bias potential V_b of the probes such that it either collects electrons when the potential is positive, or positively charged ions when the potential is negative. In the so-called sweep mode, the bias potential of the probe is swept from a minimum of −32 V to a maximum +32 V over a time period of a few milliseconds. Such sweeps are typically carried out with a cadence of ∼3 minutes. The sweep voltage range varied throughout the mission but from 2015 January, the voltage sweep usually covered most of the ±32 V range and we therefore only use the LAP data from 2015 January 1 until end of the mission on 2016 September 30.

From the current–voltage (I–V) curve, plasma parameters such as the electron density, n_e, and temperature, T_e, can be estimated. In the orbit motion limited (OML) framework (Mott-Smith & Langmuir 1926; Medicus 1962; Fahleson et al. 1974), when the probe sphere radius is smaller than the Debye length of the plasma, the electron current collected by the probe at a positive potential can be expressed as

$$I_e = An_e e\sqrt{\frac{KT_e}{2\pi m_e}}\left(1+\frac{eU}{KT_e}\right), \tag{2}$$

where $A = 4\pi a^2$ is the area of the probe with a radius of $a = 0.025$ m, e is the electron charge, K is Boltzmann's constant, m_e the electron mass, and $U = V_b - V_s$ the probe potential with respect to the plasma, which differs from the bias potential, V_b, by the spacecraft potential, V_s.

The derivative of the electron current with respect to the probe potential is

$$\frac{dI_e}{dU} = a^2 n_e e^2\sqrt{\frac{8\pi}{m_e KT_e}}, \tag{3}$$

and is referred to as the electron slope, proportional to both n_e and to $1/\sqrt{T_e}$. In a statistical study, Engelhardt et al. (2018) used the measured electron slope combined with independent n_e measurements from the mutual impedance probe (MIP; Trotignon et al. 2007) to determine T_e throughout the *Rosetta* mission. Their findings suggest the that the electron gas typically consists of two populations, one warmer and one colder, with temperature distributions centered around 0.1 eV and 10 eV, respectively. When a significant fraction of the electrons ($\gtrsim$20%) belongs to the cold population, very steep LAP slopes where found. Mission-wide statistics showed that for practical purposes a slope greater than ∼70 nA V^{-1} is a clear indicator of such a cold component. This provided a useful proxy method for determining if there are cold electrons present or not: they are present if the slope of the measured I–V curve is above 70 nA V^{-1}. It can be noted that MIP is also capable of independently detecting cold electrons (Gilet et al. 2017), which have been used in this paper only to validate our results.

Due to the lack of a proper upstream monitor, using *Rosetta* magnetic field measurements is the best available option for inferring the interplanetary magnetic field (IMF) orientation in the vicinity of the comet, on a statistical level. To determine the direction of the solar wind convective electric field from Equation (1) we use measurements of the magnetic field, at a cadence of 1 s from the MAG instrument, combined with the assumption of a solar wind velocity strictly in the $-x_{\mathrm{CSEQ}}$ direction. The measured magnetic field inside the coma of the comet will not be the same as the IMF in the undisturbed solar wind, but our study is based on the assumption that it is the solar wind convective electric field, outside the coma, that acts as a boundary condition for the plasma environment in the coma. In order to minimize errors caused by an uncertainty in the calibration of the instrument we only use the MAG data when the magnitude of the field in the y–z plane is larger than 10 nT. The assumption of a strictly radial solar wind velocity means that we only get the composant of the convective electric field in y–z plane and can ignore the x_{CSEQ} component of the magnetic field. Assuming that the draping mainly takes place in the plane containing the solar wind flow direction and the IMF, the cone angle of the IMF ($arccos(b_x/|B|)$) will change but the clock angle, measured from the $+y_{\mathrm{CSEQ}}$-axis toward $+z_{\mathrm{CSEQ}}$, will stay constant. Figure 1(a) shows a schematic of the definitions of the clock and cone angles. We illustrate the changing of these angles due to the draping in Figure 2 where we have plotted the orientation of the magnetic field as measured by *Rosetta* at 67P in comparison to that measured by the *Wind* spacecraft at Earth's L1 Lagrange point. The clock angle has a roughly similar distribution at Earth as at *Rosetta*, while the distribution of the cone angle does indeed differ more. The magnetic field measurements at Earth and *Rosetta* are from different heliospheric longitudes and radial distances and no extrapolation or time shift has been applied to these

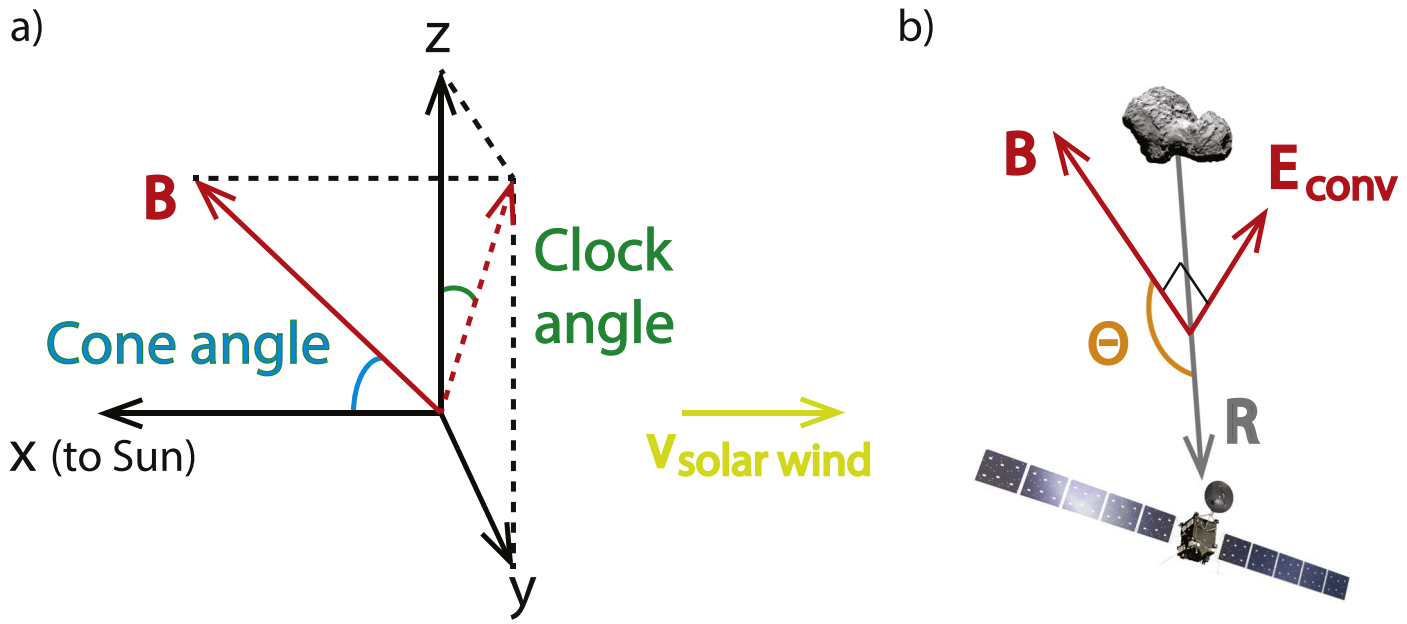

Figure 1. (a) Schematic showing the clock angle and cone angle of the interplanetary magnetic field **B** in the CSEQ reference frame, and (b) the angle θ between $\boldsymbol{E}_{\rm conv}$ and the position vector $\boldsymbol{R}$ of *Rosetta*.

data, so the distribution only represents a statistical mean over a 1.5 yr interval.

3. Results

To study the cold plasma distribution with the convective electric field direction, we begin by calculating angle θ between *Rosetta*'s position vector and the convective electric field vector in the y–z plane. The definition of angle θ is illustrated in Figure 1(b) and indicates where *Rosetta* is located with respect to the local direction of the convective electric field. For instance, $\theta = 0^\circ$ means that $+\boldsymbol{E}_{\rm conv}$ is pointing in the direction from the comet nucleus to *Rosetta* and $\theta = \pm 180^\circ$ means that $+\boldsymbol{E}_{\rm conv}$ is pointing in the direction away from *Rosetta*. θ can therefore be seen as a clock angle in the CSE reference frame.

In Figure 3(a) we show the distribution of the LAP sweep measurement with respect to the angle θ. We only include data from when a reliable electron slope could be retrieved, from 2015 January 1 to 2016 September 30, when the voltage sweep range was the same, when the magnetic field projected on the y–z plane was larger than 10 nT, and when *Rosetta* was within 500 km from the nucleus. The heliocentric distance changed from 2.6 au on 2015 January 1 to 1.2 au at perihelion on 2015 August 13 and increased from there to 3.8 au on 2016 September 30. to There is a sinusoidal variation added to the distribution which comes from the IMF nonuniform distribution in the y–z plane (see Figure 2(b)) in combination with the fact that *Rosetta* spent more time in certain locations around the nucleus than other. *Rosetta* was more often located in the $-y_{\rm CSEQ}$ hemisphere than in the $+y_{\rm CSEQ}$ hemisphere, for instance.

In Figure 3(b), we show the distribution of only the cold plasma detections, i.e., the LAP sweeps from which we identify the presence of cold plasma based on the value of the electron slope. These are much fewer in number (about 9%), as indicated in the panels, and have a different distribution. Figure 3(c) shows the relative distribution of the cold plasma, i.e., the number of LAP cold plasma detections divided by all LAP measurements (panel b divided by panel a). As can be seen, there is a a higher fraction of sweeps with cold plasma detected in the direction of $\pm 180^\circ$, which is in the direction of the $-\boldsymbol{E}_{\rm conv}$ hemisphere. Roughly 30% of all measurements indicate the presence of cold electrons when at $\pm 180^\circ$, while cold electrons are only detected in about 15% of the measurements when *Rosetta* is located in the $+\boldsymbol{E}_{\rm conv}$ hemisphere ($-90^\circ < \theta < 90^\circ$). We may note here that very similar results are obtained if we use cold plasma measurements from MIP instead of from LAP.

In Figure 3(d) we illustrate the same point in an alternative way, by plotting the fraction of cold plasma measurements as a 2D histogram in the CSE frame, noting that the convective electric field direction is parallel to the $+z_{\rm CSE}$ direction. The LAP measurements are grouped in 60×60 km bins and the fraction of cold plasma detections to the total number of measurements in each bin is calculated. As can be seen quite clearly, there is a preference for cold electrons to be detected more often in the $-\boldsymbol{E}_{\rm conv}$ hemisphere ($z_{\rm CSE} < 0$), consistent with Figure 3(c). Closer to the nucleus, this preference is less articulated, which makes sense given that the inner part of the coma should be, to some extent at least, shielded by the solar wind convective electric field.

Rather than looking at the distribution with respect to the convective electric field, we show in Figure 4 the fraction of cold plasma detections with respect to angle θ_B, i.e., the angle between *Rosetta*'s position vector and the orientation of the magnetic field vector (but now not projected onto the $y-z$ plane). This figure could potentially reveal that cold electrons are more prone to travel along magnetic field lines, if a larger fraction of sweeps with cold electron signatures were observed when the magnetic field was in the direction from (toward) the nucleus to (from) *Rosetta*. However, if any, there seems to be a broad peak centered around an angle of 90°, i.e., when the magnetic field vector is perpendicular to *Rosetta*'s position vector. This is a strong indication that the convective electric field is more important than the local magnetic field for the cold plasma distribution.

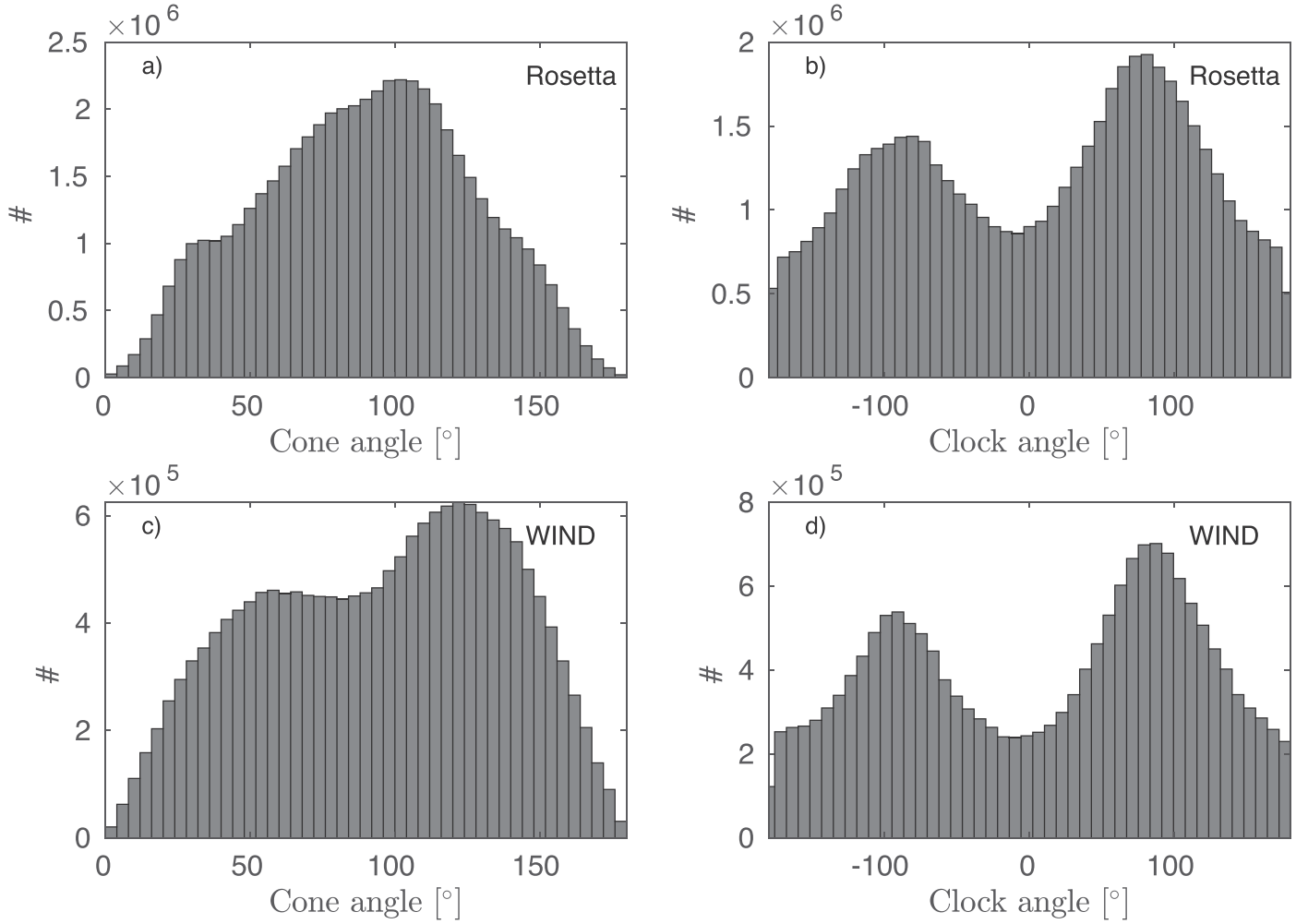

Figure 2. Orientation of the magnetic field (cone angle and clock angle) at *Rosetta*'s location compared to the IMF orientation at Earth from 2015 January 1 to 2016 October 1.

Related to the presence of cold electrons is also the presence of a diamagnetic cavity. For instance, Odelstad et al. (2018) showed that cold plasma is always found inside the diamagnetic cavity, while the cold plasma is more sporadically detected outside of it. Motivated by this we have in a similar way tested if the appearance of the diamagnetic cavity is linked to the orientation of the convective electric field. To determine the orientation of the magnetic field and convective electric field during the cavity detection we use magnetic field measurements 1 minute before each cavity detection and take the average field orientation during that interval (expanding this to an average over 5 minutes, before as well as after a cavity observation, made no significant difference to the results). We then calculate the convective electric field direction and angle θ to *Rosetta*'s position vector at the time of a cavity detection in the same way as before. In Figure 5 we show the normalized fraction of diamagnetic cavity detections as a function of θ to see if it is preferably found at any specific θ. To get the fraction of cavity observations we divide the number of cavity detections with the total number of observations in that θ direction, similar to what was done in Figure 3(a). We then normalize to the maximum value of the distribution. It can be seen that the distribution of the detections of the diamagnetic cavity with respect to θ is similar to the distribution of the cold plasma detections (see Figure 3(a)), and the cavity is more often found when in the $-\boldsymbol{E}_{\rm conv}$ hemisphere with a noticeable secondary peak around 0°.

4. Conclusions and Discussion

We have shown that the cold (<1 eV) plasma around comet 67P, as detected by LAP, is dependent on the direction of the convective electric field, as determined by local measurements of the magnetic field by MAG, combined with an assumption of a purely radial solar wind flow (Figure 3). The cold plasma is more often found in the $-\boldsymbol{E}_{\rm conv}$ hemisphere, which is interpreted as the cold electrons being affected by this electric field on a global scale. We note here that Masunaga et al. (2019) found that ions above 40 eV in and around the diamagnetic cavity also move in the direction of $-\boldsymbol{E}_{\rm conv}$. A suggestion was that these antisunward flowing cometary ions inside the solar wind ion cavity were mass-loaded by newly added plasma, and so they behaved like the solar wind further out. Otherwise, cometary ions are typically moving radially away from the nucleus in the y–z plane, irrespective of the direction of $\boldsymbol{E}_{\rm conv}$ (Nilsson et al. 2017; Bercic et al. 2018), in agreement with a strong shielding of the inner coma from the solar wind electric field (Nilsson et al. 2018). It is therefore very interesting that the $\boldsymbol{E}_{\rm conv}$ affects the distribution of cold electrons as well as the ions near the diamagnetic cavity.

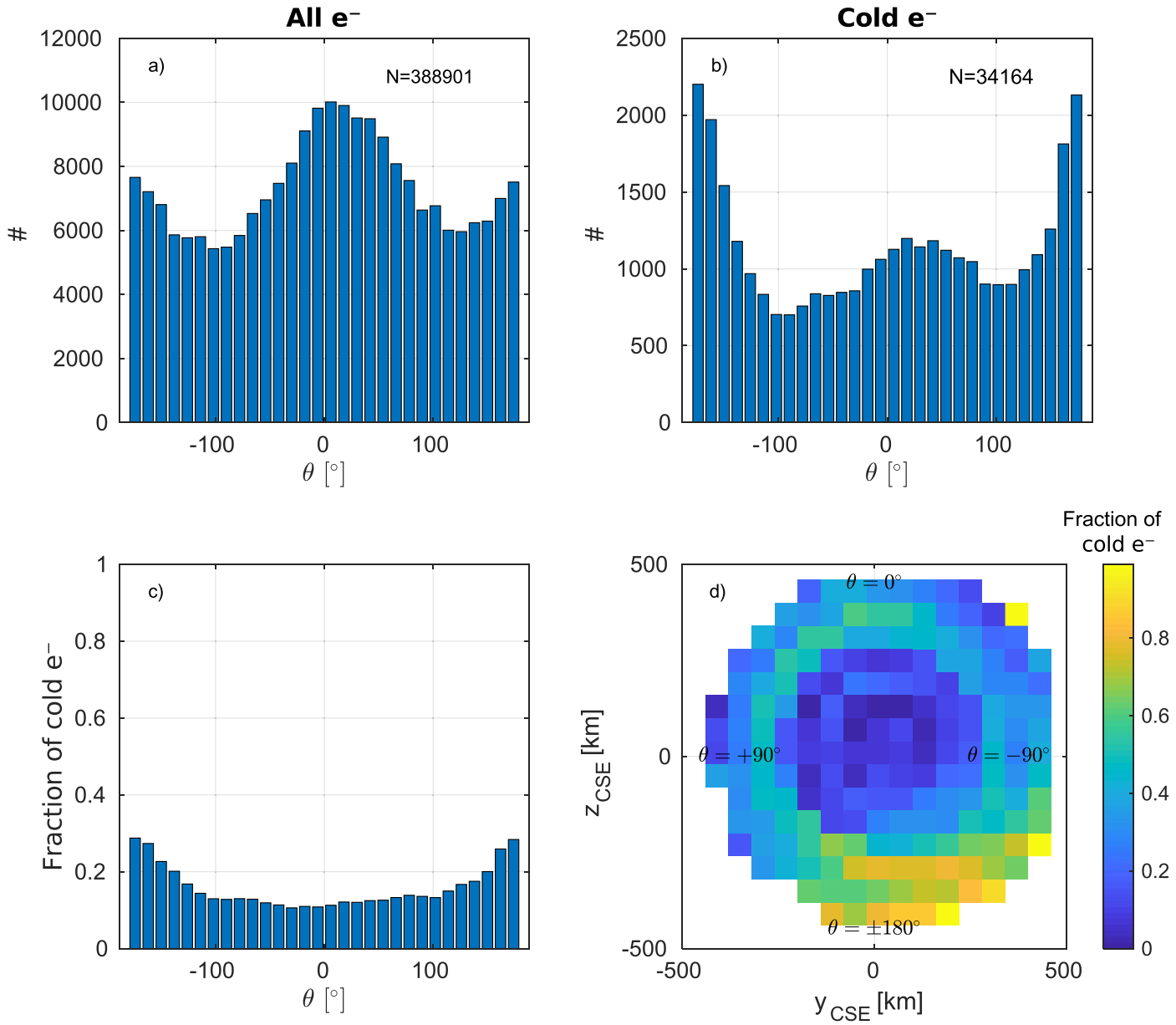

Figure 3. Distribution of (a) the total number of observations, LAP sweeps, with respect to the angle θ, i.e., the angle between the convective electric field direction and *Rosetta*'s position vector, (b) the number of cold plasma observations with respect to θ, (c) the fraction of cold plasma observations to the total number of observations with respect to θ, and (d) a 2D histogram showing the fraction of cold plasma observations with respect to the $z_{\rm CSE}$ and $y_{\rm CSE}$ coordinates. The angle $\theta \in [-180°, 180°]$ is defined as positive in the counterclockwise direction, as indicated in panel d. $\boldsymbol{E}_{\rm conv}$ is directly parallel to $+z_{CSE}$ in panel d.

The cold electrons are shown to not predominately follow and be accelerated along the magnetic field lines as the distribution of the cold plasma detections with respect to the magnetic field direction were not correlated (Figure 4). Furthermore, a detection of a diamagnetic cavity is roughly twice as likely when *Rosetta* is located in the $-\boldsymbol{E}_{\rm conv}$ hemisphere compared to when in the $+\boldsymbol{E}_{\rm conv}$ hemisphere, where it in turn is 50% more likely to be detected than when aligned with the magnetic field. This suggests circumstantially that the cavity's existence is related to the presence of cold electrons. Previous simulations also indicate that the diamagnetic cavity is generally shifted in the $-\boldsymbol{E}_{\rm conv}$ direction (Koenders et al. 2015). The secondary peak of the diamagnetic cavity distribution around 0° (Figure 5) is very much consistent with the cavity shape seen in multifluid Hall magnetohydrodynamic simulations by Huang et al. (2018). While for instance an ambipolar electric field, set up by a charge separation between electrons and ions, also modifies the plasma environment (e.g., Madanian et al. 2016; Vigren et al. 2017; Bercic et al. 2018), the solar wind convective electric field seems to have an overarching influence.

A number of assumptions are included in this study which need to be emphasized: the solar wind is assumed to be purely radial, which is probably not too far from the truth outside the comet, but as soon as it interacts with the comet, strong shears in the ion flow have been observed (Behar et al. 2016). Our study is hence relying on that it is the solar wind convection electric field at large that sets the boundary condition for the cometary plasma in this respect, rather than any field generated within the coma. The assumption that the IMF, projected on the y–z plane, having the same orientation as the magnetic field measured inside the cometary plasma environment is another

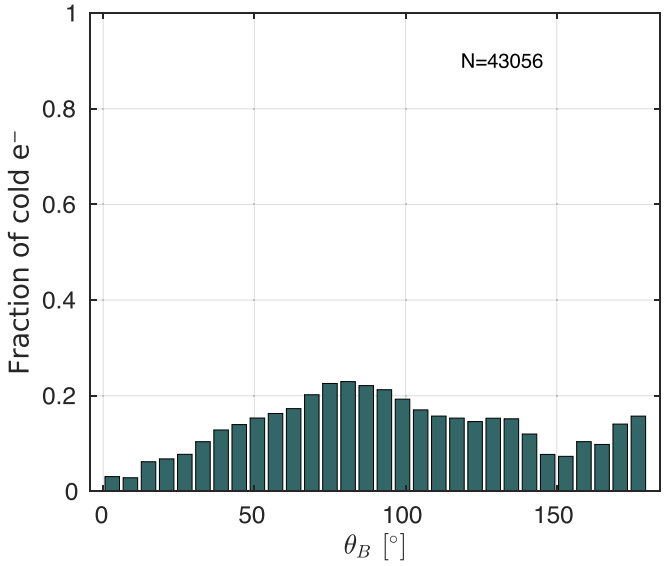

Figure 4. Distribution of the fraction of cold plasma observations to the total number of observations with respect to θ_B, i.e., the angle between the magnetic field vector and *Rosetta*'s position vector.

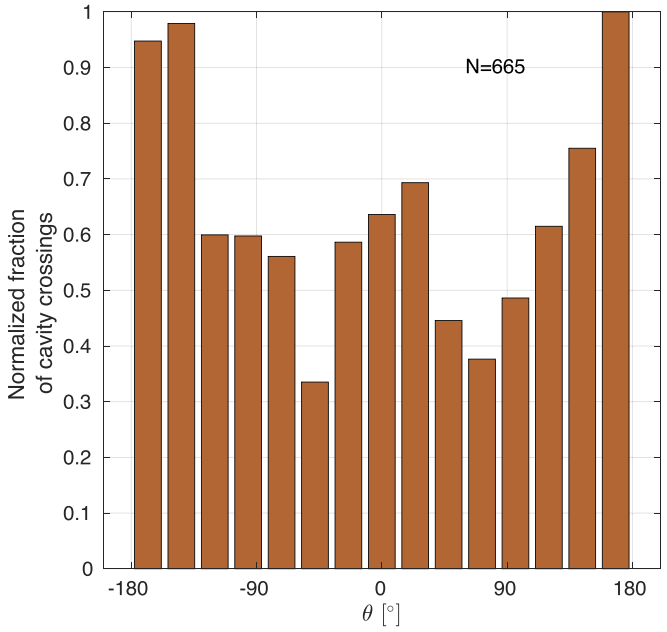

Figure 5. Normalized distribution of the fraction of diamagnetic cavity observations as a function of angle θ. The diamagnetic cavity is more often present in the $-\boldsymbol{E}_{\rm conv}$ hemisphere, similar to the cold electrons.

source of error here. Still, comparison between *Rosetta* and *Wind* data from Earth's orbit show vary similar distributions of the IMF angle on a statistical level. We also assume that most of the cometary plasma detected is coming from a region in between *Rosetta* and the nucleus, as opposed to being ionized elsewhere in the coma and then transported to *Rosetta* along some other path. This is however a reasonable assumption given that the neutrals expand radially and the plasma stem from the ionization of these neutrals.

In summary, our results suggest that the solar wind convective electric field has an effect on the plasma environment all the way down to the diamagnetic cavity (in agreement with the findings of Masunaga et al. (2019)). The cold plasma as well as the diamagnetic cavity are preferably found in the $-\boldsymbol{E}_{\rm conv}$ hemisphere.

Rosetta is a European Space Agency (ESA) mission with contributions from its member states and the National Aeronautics and Space Administration (NASA). The work on the RPC-LAP data was funded by the Swedish National Space Board under contracts 109/12 and 135/13 and Vetenskapsrådet under contracts 621-2013-4191 and 621-2014-5526. Work at LPC2E/CNRS was supported by CNES and by ANR under the financial agreement ANR-15-CE31-0009-01.

ORCID iDs

Niklas J. T. Edberg https://orcid.org/0000-0002-1261-7580
Erik Vigren https://orcid.org/0000-0003-2647-8259

References

André, M., Odelstad, E., Graham, D. B., et al. 2017, MNRAS, 469, S29
Behar, E., Nilsson, H., Wieser, G. S., et al. 2016, GeoRL, 43, 1411
Bercic, L., Behar, E., Nilsson, H., et al. 2018, A&A, 613, A57
Biermann, L., Brosowski, B., & Schmidt, H. 1967, SoPh, 1, 254
Broiles, T. W., Burch, J. L., Chae, K., et al. 2016, MNRAS, 462, S312
Broiles, T. W., Burch, J. L., Clark, G., et al. 2015, A&A, 583, A21
Broiles, T. W., Livadiotis, G., Burch, J. L., et al. 2016, JGRA, 121, 7407
Cravens, T. E., Kozyra, J. U., Nagy, A. F., Gombosi, T. I., & Kurtz, M. 1987, JGRA, 92, 7341
Deca, J., Divin, A., Henri, P., et al. 2017, PhRvL, 118, 205101
Edberg, N. J. T., Alho, M., André, M., et al. 2016a, MNRAS, 462, S45
Edberg, N. J. T., Eriksson, A. I., Odelstad, E., et al. 2015, GeoRL, 42, 4263
Edberg, N. J. T., Eriksson, A. I., Odelstad, E., et al. 2016b, JGRA, 121, 949
Engelhardt, I. A. D., Eriksson, A. I., Vigren, E., et al. 2018, A&A, 616, A51
Eriksson, A. I., Boström, R., Gill, R., et al. 2007, SSRv, 128, 729
Eriksson, A. I., Engelhardt, I. A. D., André, M., et al. 2017, A&A, 605, A15
Fahleson, U., Fälthammar, C., & Pedersen, A. 1974, P&SS, 22, 41
Gilet, N., Henri, P., Wattieaux, G., Cilibrasi, M., & Béghin, C. 2017, RaSc, 52, 1432
Glassmeier, K.-H., Richter, I., Diedrich, A., et al. 2007, SSRv, 128, 649
Goetz, C., Koenders, C., Richter, I., et al. 2016, A&A, 588, A24
Henri, P., Vallières, X., Hajra, R., et al. 2017, MNRAS, 469, S372
Heritier, K. L., Galand, M., Henri, P., et al. 2018, A&A, 618, A77
Huang, Z., Tóth, G., Gombosi, T. I., et al. 2018, MNRAS, 475, 2835
Johansson, F. L., Odelstad, E., Paulsson, J. J. P., et al. 2017, MNRAS, 469, S626
Karlsson, T., Eriksson, A. I., Odelstad, E., et al. 2017, GeoRL, 44, 1641
Koenders, C., Glassmeier, K.-H., Richter, I., Ranocha, H., & Motschmann, U. 2015, P&SS, 105, 101
Madanian, H., Cravens, T. E., Richard, M. S., et al. 2016, JGRA, 121, 8013
Masunaga, K., Nilsson, H., Behar, E., et al. 2019, A&A, submitted
Medicus, G. 1962, JAP, 33, 3094
Mott-Smith, H. M., & Langmuir, I. 1926, PhRv, 28, 727
Nilsson, H., Gunell, H., Karlsson, T., et al. 2018, A&A, 616, A50
Nilsson, H., Wieser, G. S., Behar, E., et al. 2017, MNRAS, 469, S252
Odelstad, E., Eriksson, A. I., Johansson, F. L., et al. 2018, JGRA, 123, 5870
Simon Wedlund, C., Alho, M., Gronoff, G., et al. 2017, A&A, 604, A73
Timar, A., Nemeth, Z., Szego, K., et al. 2017, MNRAS, 469, S723
Trotignon, J. G., Michau, J. L., Lagoutte, D., et al. 2007, SSRv, 128, 713
Vigren, E., André, M., Edberg, N. J. T., et al. 2017, MNRAS, 469, S142
Vigren, E., & Eriksson, A. I. 2019, MNRAS, 482, 1937